PROPERTIES OF HIGH-ENTROPIC FECOCRNITATIMO COATINGS

[1]Yurov V.M.,
[2]Salkeeva A.K.,
[2]Kusenova A.S.
[1]Karaganda University named after E.A. Buketov
[2]Karaganda Technical University
Kazakhstan, Karaganda

Abstract. The FeCoCrNiTaTiMo alloy and coatings based on it have been synthesized by mechanical alloying. - The optical microstructure of high-entropy coatings exhibits irregularity, which is clearly visible on the maps of energy-dispersive spectroscopy. XPS spectra indicate the formation of high-entropy coatings. Analysis of the elemental composition shows the complexity of the high-entropy alloy FeCoCrNiTaTiMo. The structure consists of solid solutions with a chaotic arrangement of atoms of elements. The microhardness of our coating (345 HV) is not inferior to stainless steels, and the wear resistance of the coating is $3 \cdot 10^{-4}$ g/min. High-entropy FeCoCrNiTaTiMo coatings turn out to be antifrictional, which obviously leads to energy savings. The thickness of the surface layer d(I) is determined by one fundamental parameter - the molar (atomic) volume of the element and is equal to 12.3 nm. it is shown that the formation of a cellular nanostructure in a coating can ocMor according to several models.

Key words: high-entropy alloy, plasma coating, surface layer, microhardness, friction, wear resistance, wear resistance of the coating.

Introduction

According to the authors of [1], a distinctive feature of high-entropy alloys (HEAs) from traditional ones is that these alloys have a high entropy of mixing, which affects the formation of structures based on solid solutions. A little over 15 years have passed since the discovery of high-entropy alloys (2004). The first review was made as a complete material science cycle "production - structure - properties" for a new class of vacuum-plasma coatings - nitrides of multielement metal high-entropy alloys in [2]. An analysis was made of the current state of obtaining such coatings, their morphology, elemental and phase compositions, structure, substructure, stress state, and functional properties depending on the main formation parameters: substrate temperature during deposition, the magnitude of the bias potential applied to the substrate, and the composition of the gas atmosphere. Then there were many works devoted to the synthesis and study of various HEAs [3-9]. The last review on HEAs was made in [10]. The analysis of more than 200 obtained high-entropy alloys (HEAs) made it possible to establish the relationship between the electron concentration, phase composition, lattice parameter and properties of solid solutions based on bcc and fcc lattices. The main conditions for the appearance of high-entropy chemical compounds - the Laves phase, σ- and μ-phases, are revealed. For the formation of a 100% high-entropy σ-phase, a necessary condition is that all elements that make up the HES must form a σ-phase in two-component alloys in various combinations, and the electron concentration of the alloy must be in the range of 6.7-7.3 el./at. For the formation of a 100% high-entropy Laves phase, it is necessary to have: the total negative enthalpy of mixing of the alloy at the level of -7 kJ/mol and below; pairs with a difference in atomic sizes of more than 12 %; the presence in the alloy of two elements with an enthalpy of mixing less than -30 kJ/mol, the average electron concentration should be in the range of 6-7 el./at. It is shown that the ratio of the lattice parameters of solid-solution HES, determined in the experiment, to the lattice parameter of the most refractory metal in the HES determines the value of the elastic modulus.

In this work, the physicomechanical properties of the high-entropy FeCoCrNiTaTiMo coating synthesized by us are investigated.

Methods for the synthesis of the FeCoCrNiTaTiMo alloy and coatings.

To prepare the tablets, micropowders of the corresponding metals were taken (Fig. 1a) and mixed in equiatomic proportions. Then the prepared mixture of powders was placed in a grinding bowl of a planetary ball mill (Fig.1b) made of tungsten carbide, and grinding bodies (balls 5-10 mm in diameter) also made of tungsten carbide were added, the mass of which was equal to 10 masses of the powder mixture. After that, the glass was filled with Galosha gasoline, the lid was tightly closed, and the planetary ball mill was turned on (rotation speed was 500 rpm, operating time 5 hours). The homogenized compositions obtained in this way were then dried in a vacuum and, using a mold (pressure of 20 tons), were pressed into flat disks 12 mm in diameter and 3 mm thick (Fig.1c).

a) metal microstrips

b) ball mill

c) flat discs

Figure 1 - Synthesis of the FeCoCrNiTaTiMo alloy: metal micropowders (a), planetary ball mill (b), synthesized flat disks (c)

Experimental technique. In the study of the microstructure of the coatings of the samples, we used an Epiquant metallographic microscope (Fig. 2 a). This device operates on the principle of a linear analyzer and is intended for structural and analytical studies of solid, heterogeneous substances, in which physical and technological properties depend on the geometric microstructure and the structural components of which have different reflection coefficients (Fig. 2 b).

a)

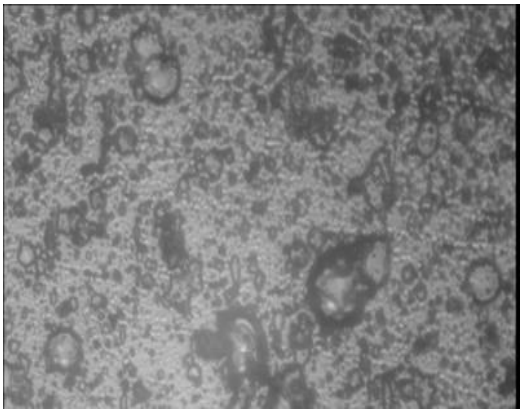

b)

Figure 2 - Microscope "Epiquant" (a), pictures of the coating (x1000) (b)

Electron microscopic examination was carried out on a JEOL JSM-5910 scanning electron microscope (Fig. 3 a). The studies were carried out at an accelerating voltage of 20 kV. For each sample, 4 images were taken from 4 points of the surface at magnifications: 245, 1060, 4500 and 14600 times (Fig. 3 b).

a)

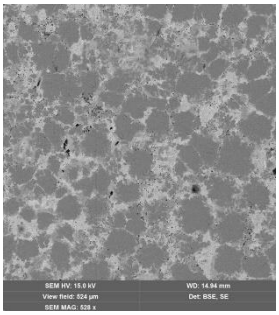

b)

Figure 3 - Microscope JEOL JSM-5910 (a) and SEM images of coatings (b)

X-ray fluorescence electron spectroscopy (XPS) was carried out using a TESCAN MIRA 3 electron microscope. The elemental composition (Fig. 4 a) and the unevenness of the elemental composition (Fig. 4 b) were determined.

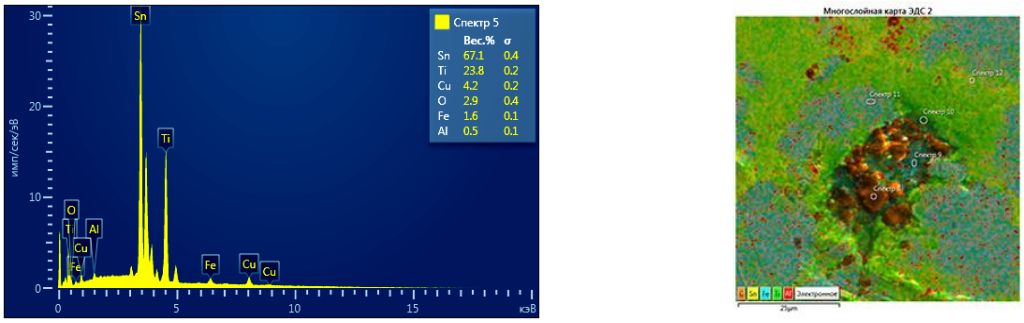

а) *б)*

Figure 4 - Elemental composition (a) and uneven elemental composition (b).

On an XRD-6000 X-ray diffractometer (Fig. 5 a), the phase composition and structure parameters of the deposited ion-plasma coating were studied (Fig. 5 b).

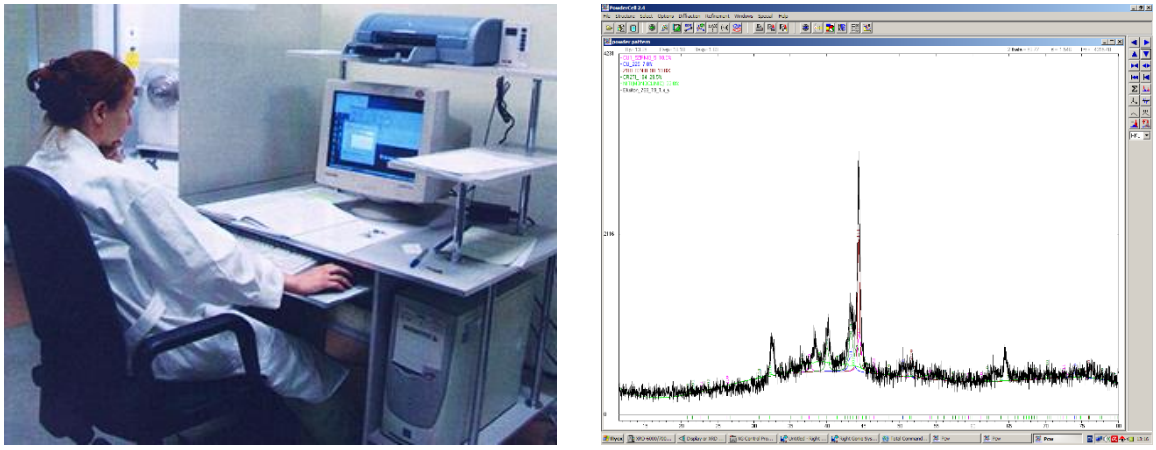

а) *b)*

Figure 5 - XRD-6000 diffractometer (a) and a section of the diffractogram (b)

Система Quanta 200 3D совмещает в себе сканирующий электронный микроскоп с термоэмиссионным катодом (рис. 6 а), сфокусированный ионный пучок, позволяющий прецизионно наносить и удалять материалы, определяя толщину покрытия (рис. 6 б).

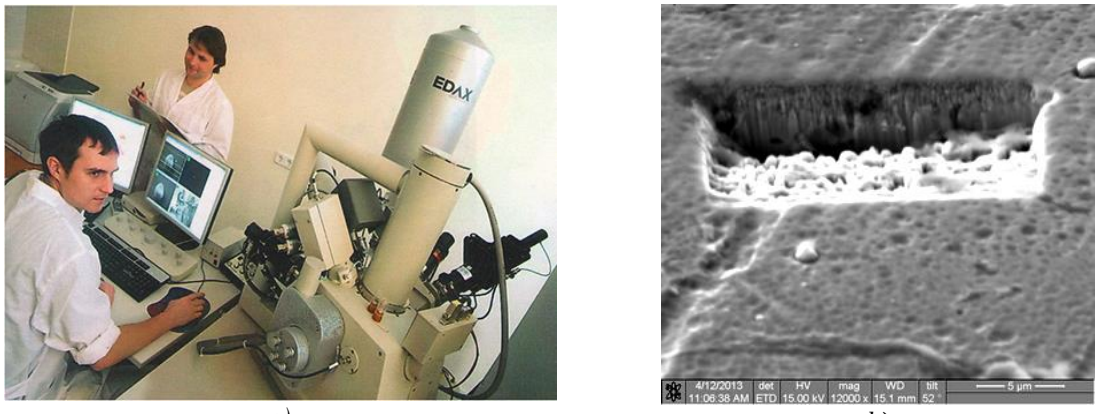

а) *b)*

Figure 6 - Quanta 200 3D system (a) and coating thickness (b)

Investigation of the morphology (Fig. 7 b) of the surface of the films obtained by thermal evaporation in a vacuum was carried out on a JSPM-5400 atomic force microscope (AFM) manufactured by JEOL (Fig. 7 a).

a)

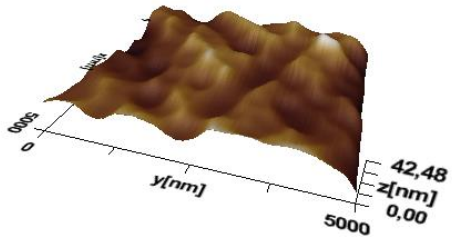

b)

Figure 7 - AFM JSPM-5400 (a) and 3D - coating surface (b)

The experimental setup for determining the friction coefficients was built by us on the principle of modularity. The general scheme of the installation for determining the friction coefficients is shown in Fig. 8 a, and the appearance of the graphical presentation of research results using the system is shown in Fig. 8 b.

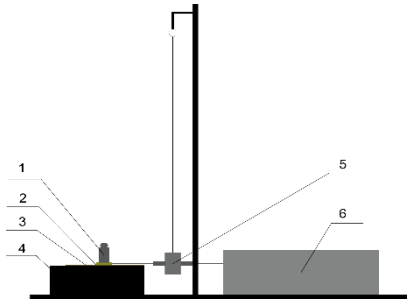

1 - known clamping weight, 2 - sample, 3 - sliding surface, 4 - measuring table, 5 - force transducer, 6 - electronics unit and drive

a)

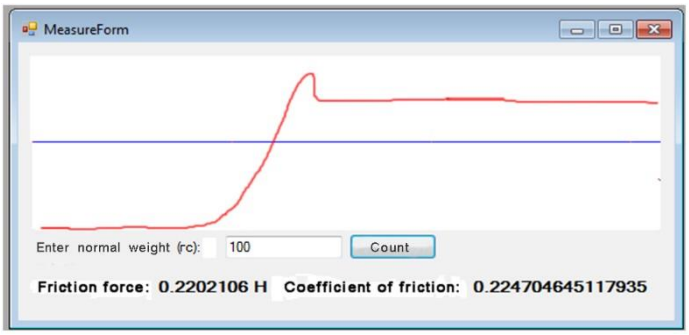

b)

Figure 8 - General scheme of the installation (a) and the type of graphical representation research results (b)

We used the method of testing for microabrasive wear by the action of a rotating steel ball on a flat sample with the addition of an emulsion containing abrasive particles (Fig. 9 b). A spherical crater, called a calotte, is formed at the point of contact; therefore, the device for this type of testing was called a caloteter (Fig. 9 a).

a)

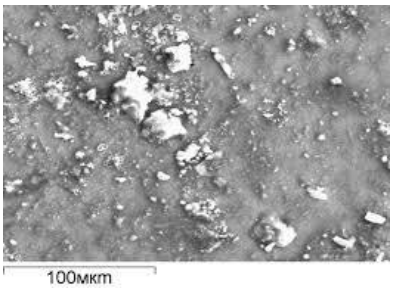

b)

Figure 9 - Calotester device (a) and wear test (b)

The control of coatings for hardness was carried out on an HVC-1000A electronic microhardness meter (Fig. 10 a). The results are shown in Fig. 10 b.

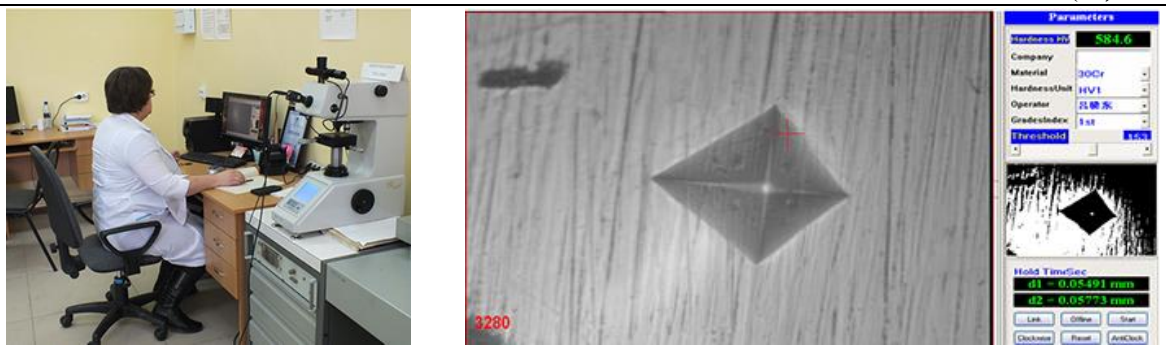

a) *b)*

Figure 10 - Microhardness meter HVC-1000A (a) and the result (b)

Structure of FeCoCrNiTaTiMo coatings. In fig. 11 shows the optical microstructure of high-entropy (HES) FeCoCrNiTaTiMo coatings at two points. The unevenness of the coating is observed, which is clearly visible on the maps of energy dispersive spectroscopy (emf) of this coating (Fig. 12).

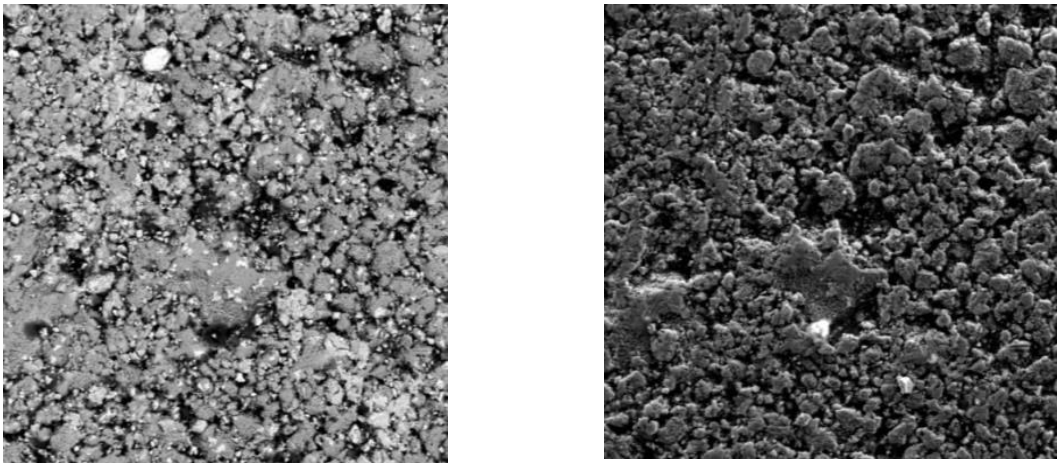

Figure 11 - Optical microstructure of FeCoCrNiTaTiMo coatings

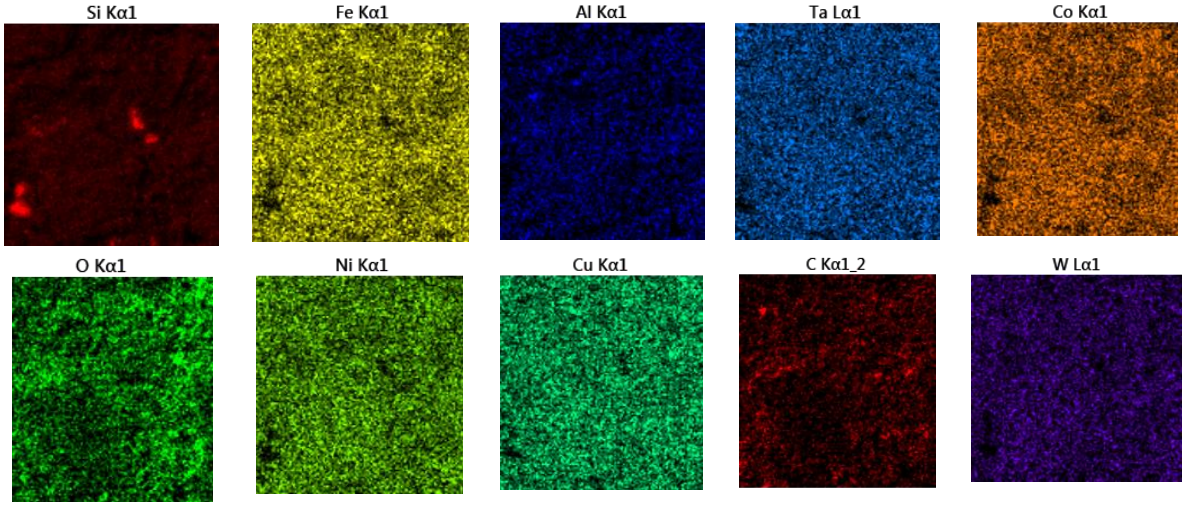

Figure 12 - Energy dispersive spectroscopy FeCoCrNiTaTiMo

The distribution maps of elements (Fig. 12) show the nonequilibrium of the chemical elements Fe, Co, Mo in comparison with the elements Ta, Cr, Ni. The concentration of other elements is negligible. The XPS spectra shown in Fig. 13 and in table. 1 indicate the formation of high-entropy coatings.

Table 1

Chemical composition in% FeCoCrNiTaTiMo

Fe	Co	Cr	Ni	Ta	Ti	Mo
17	18	16	16	18	16	9

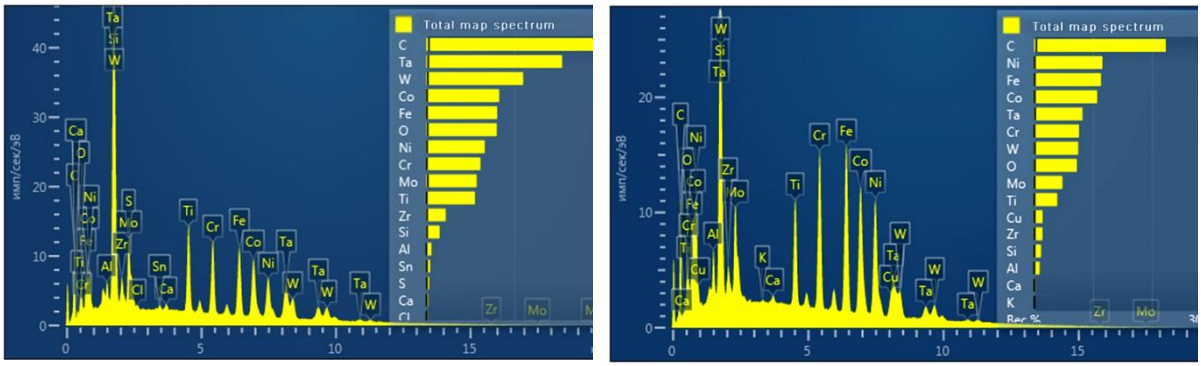

Figure 13 - XPS spectra FeCoCrNiTaTiMo

The content in the spectra in Fig. 12 and 13 elements of tungsten are quite noticeable. It was not added in our metal micropowders, but appeared in the process of grinding the powders with tungsten carbide balls. In fig. 14 shows PEM FeCoCrNiTaTiMo.

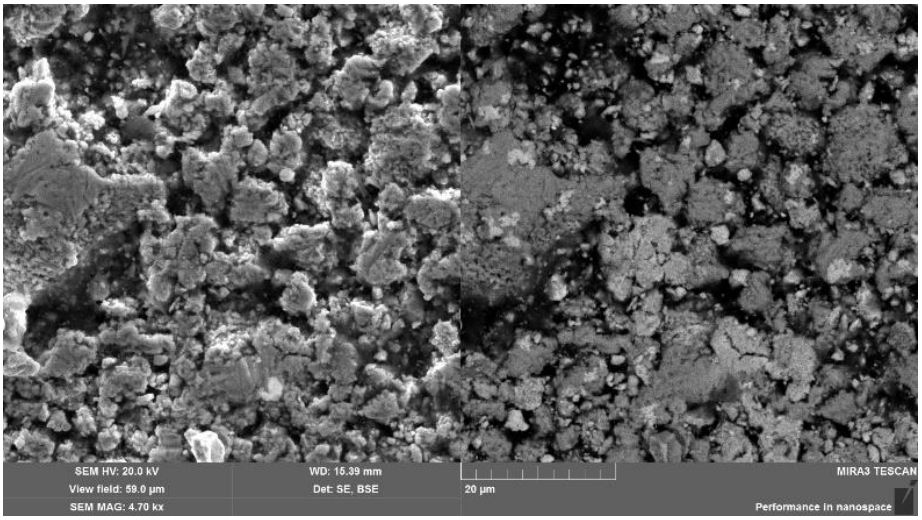

Figure 14 - PEM coating FeCoCrNiTaTiMo

Studies have shown that the alloy of the FeCoCrNiTaTiMo system consists of large elongated grains with an average width of 100-150 μm and an average length of 200-300 μm. It should be noted that black precipitates about 5-7 microns in size are observed in the alloys. According to the literature data, these precipitates are oxides (Me_2O_3). In the course of the study, more complex structural components were discovered. The inner part of the grains of the alloys is similar to the eutectoid structure. The grains are separated by thick layers of the second phase.

In fig. 15 shows the diffraction pattern of the FeCoCrNiTaTiMo coating. Phases are present: Fe, Ti, $TaFe_2$, possibly the presence of phases $TaCo_2$, Mo, Ti, Ni_2Ti, TaCrNi, TiCr, TiNi, Fe_5Ta_3.

Special tantalum alloys are used in industry for high temperature applications, for making cutters with high cutting speeds and for making acid-resistant hardware. The presence of cobalt in high-speed steels does not increase their hardness, but shifts the temperature of the onset of hardness loss to 600 °C, while in ordinary steel it decreases from 200 °C. Cobalt is also widely used to obtain magnetic materials with high magnetic permeability and alloys for permanent magnets (alloys of cobalt with iron, platinum; alloys based on cobalt, alloyed with aluminum, nickel, copper, titanium, samarium, lanthanum, cerium).

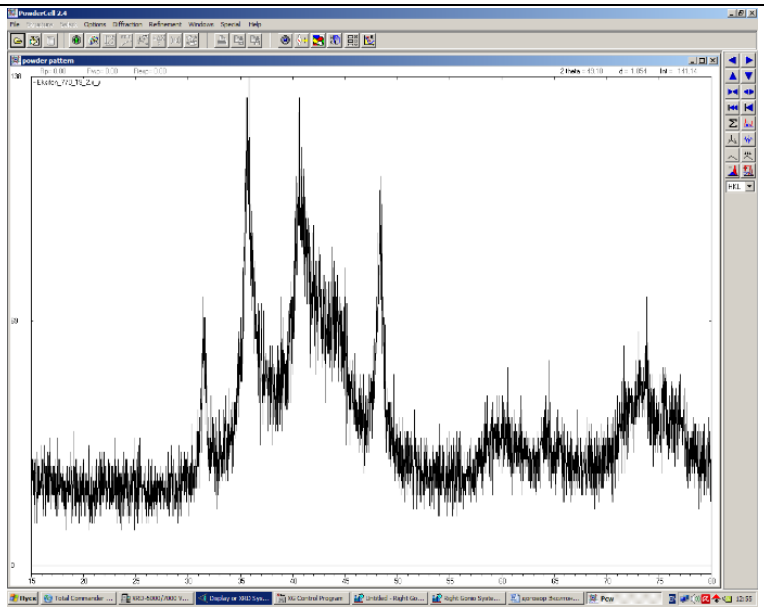

Figure 15 - Diffraction pattern of FeCoCrNiTaTiMo coating

The introduction of cobalt additives into the alloys in the amount of 0.5-4.0% helps to reduce the grain size, due to which the coercive force (demagnetization resistance) and residual magnetization increase. Industrial alloys for "alnico" magnets contain aluminum, nickel, cobalt, the rest of iron. Certain alloys also include copper and titanium.

An analysis of the elemental composition (Fig. 13-15) shows the complexity of the high-entropy FeCoCrNiTaTiMo alloy. The structure of seven-atomic high-entropy alloys consists of solid solutions with a chaotic arrangement of element atoms. It is assumed that lattice distortions due to doping with atoms of different sorts is one of the reasons for the stability of the structures of solid solutions at higher temperatures than intermetallic compounds.

Microhardness of coatings. The results of measurements of the microhardness of the FeCoCrNiTaTiMo coatings are given in Table 2.

Table 2

Microhardness of the FeCoCrNiTaTiMo coating in argon

Microhardness	1	2	3	4	5	6	7	8	**The average**
HV	342	292	299	292	370	298	265	331	**307**

Comparative data on the values of microhardness (HV) of high-entropy equiatomic and traditional alloys (for example, typical high-strength stainless steels and alloys of nickel, cobalt or titanium) are given in table. 3. The microhardness of our FeCoCrNiTaTiMo coating (Table 2) is not inferior to stainless steels.

Table 3

Microhardness of stainless steels

Alloy	Microhardness, HV	Alloy	Microhardness, HV
X18H9T	186	20XH	260
316 Stainless steel	189	Hastelloy C	236
IIIX15	200	17-4 PH Stainless steel	362
X12M	225	Stellite 6	413

Wear resistance of coatings. The results of studies of the wear resistance of FeCoCrNiTaTiMo coatings are shown in Table 4.

Table 4

Wear resistance of FeCoCrNiTaTiMo coatings

Sample wear (weight in grams) for 30 min						
Before	15,14852	15,14857	15,14859	15,14856	The average	15,148566
After	15,14745	15,14763	15,14759	15,14759	Difference	0,000986

Table 4 shows the wear resistance of the FeCoCrNiTaTiMo coating ~ $3x10^{-4}$ g/min.

Tribological features of FeCoCrNiTaTiMo coatings. The deposition of FeCoCrNiTaTiMo was carried out on a stationary sample for an hour with a reference voltage of 150 and 250 volts in a constant power mode of 1.5 kW.

Table 5

Coefficients of friction for copper and aluminum

coatings	on copper		for aluminum	
	coefficient of friction	error	coefficient of friction	error
FeCoCrNiTaTiMo	0,256	0,006	0,278	0,002

High-entropy coatings FeCoCrNiTaTiMo turn out to be antifriction, which obviously leads to energy savings. The surface layer of high-entropy coatings FeCoCrNiTaTiMo. In fig. 16 shows the thickness of the deposited coating over 40 minutes. From the figure, a columnar structure is observed; it has a size of about 1.5 microns.

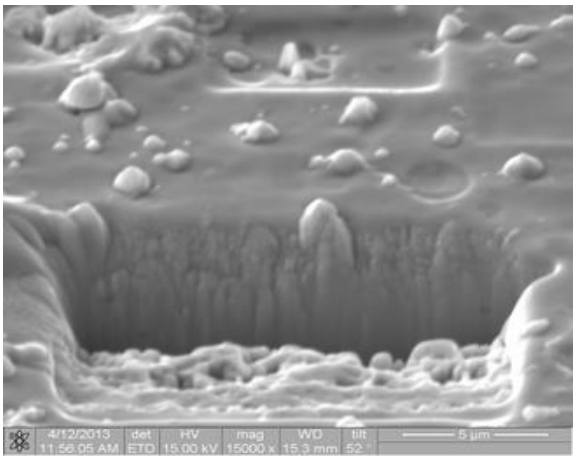

Figure 16 - Thickness of FeCoCrNiTaTiMo coating in argon gas atmosphere

In [11-13], we showed that the thickness of the surface layer d(I) is determined by one fundamental parameter - the molar (atomic) volume of an element (υ = M/ρ, M is the molar mass (g/mol), ρ is the density (g/cm^3)), which periodically changes in accordance with the table of D.I. Mendeleev:

$$d(I) = 0.17 \cdot 10^{-9} \upsilon$$

For seven-atom high-entropy FeCoCrNiTaTiMo alloys, the thickness of the surface layer will have the values given in Table 6.

Table 6

Thickness of the surface layer d FeCoCrNiTaTiMo

Alloy	ρ, g/sm^3	M, mol^{-1}	d(I), nm	d(II), nm
FeCoCrNiTaTiMo	7,15	519	14,9	149

Atomic force microscopy. In fig. 17 shows 3D images of the surface of FeCoCrNiTaTiMo coatings on AISI-201 steel samples at three different points, and below their fractal structures. The cellular structure of the high-entropy coating is observed. In [14], we gave the following explanation of this structure. Plasma deposition of coatings is a thermodynamically nonequilibrium process in an open system. The formation of a cellular nanostructure in a coating can occur according to several models:

- a cellular substructure is often formed during solidification as a result of concentration hypothermia;
- Benard cells are an example of self-organization. The control parameter of self-organization is the temperature gradient leading to a cellular substructure;
- a cellular dislocation structure is a process of self-organization of dislocations under conditions of multiple slip.

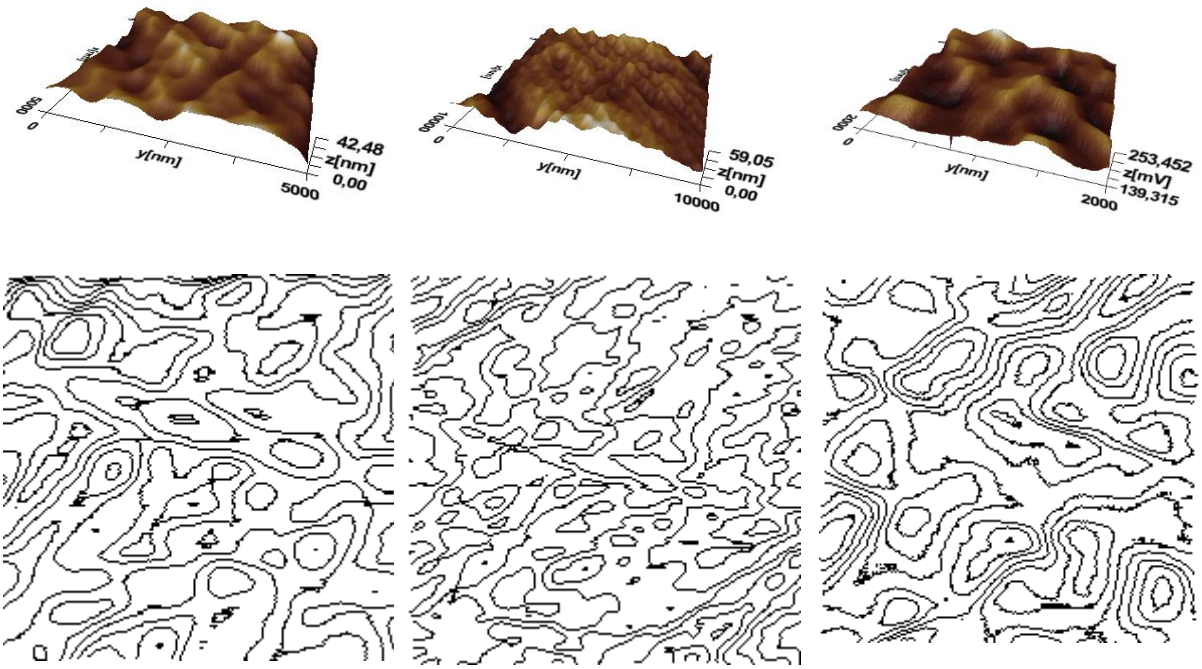

Figure 17 - 3D images of the surface of the FeCoCrNiTaTiMo coatings at three different points, and below their fractal structures.

Conclusion.

In conclusion, the following main conclusions can be drawn:

- the FeCoCrNiTaTiMo alloy and coatings based on it have been synthesized by mechanical alloying;

- the optical microstructure of high-entropy coatings reveals unevenness, which is clearly visible on the maps of energy-dispersive spectroscopy;

- XPS spectra indicate the formation of high-entropy coatings;

- analysis of the elemental composition shows the complexity of the high-entropy alloy FeCoCrNiTaTiMo. The structure consists of solid solutions with a chaotic arrangement of atoms of elements;

- the microhardness of our coating (307 HV) is not inferior to stainless steels, and the wear resistance of the coating is $3 \cdot 10^{-4}$ g/min;

- high-entropy coatings FeCoCrNiTaTiMo turn out to be antifriction, which obviously leads to energy savings;

- the thickness of the surface layer d(I) is determined by one fundamental parameter - the molar (atomic) volume of the element and is equal to 12.3 nm;

- it has been shown that the formation of a cellular nanostructure in a coating can occur according to several models.

The work was carried out under the program of the Ministry of Education and Science of the Republic of Kazakhstan. Grants № 0118RK000063 and № F.0781.

References

1. Yeh J.W., Chen Y.L., Lin S.J. High-entropy alloys – a new era of exploitation // Materials Science Forum. 2007, Vol. 560. – P. 1-9.

2. Azarenkov N.A., Sobol O.V., Beresnev V.M., Pogrebnyak A.D., Kolesnikov D.A., Turbin P.V., Toryanik I.N. Vacuum-plasma coatings based on multielement nitrides // Metallofizika and newest technologies, 2013, vol. 35, No. 8. - P. 1061-1084.

3. Firstov S.A., Gorban V.F., Krapivka N.A., Pechkovsky E.P. A new class of materials - high-entropy alloys and coatings // Vestnik TSU, 2013, v. 18, no. 4. - P. 1938-1940.

4. Firstov S.A., Gorban V.F., Andreev A.O., Krapivka N.A. Superhard coatings from high-entropy alloys // Science and Innovation, 2013, V. 9, No. 5. - P. 32-39.

5. Pogrebnyak A.D., Bagdasaryan A.A., Yakushchenko I.I., Beresnev V.M. Structure and properties of high-entropy alloys and nitride coatings based on them // Uspekhi khimii, 2014, vol. 83, no. 11, P. 1027-1061.

6. Maksimchuk I.N., Tkachenko V.G., Vovchok A.S., Medalovich N.P., Makarenko E.S. Decomposition kinetics and thermal stabilization of a cast alloy of the Mg-Al-Ca-Mn-Ti system // Metallofizika and newest technologies, 2014, vol. 36, No. 1. - P. 1-15.

7. Firstov S.A., Gorban V.F., Krapivka N.A., Pechkovsky E.P., Karpets M.V. Relationship between the σ-phase and fcc-phase and the electron concentration of cast two-phase high-entropy alloys // Composites and nanostructures, 2015, Volume 7, No. 2. - P. 72-84.

8. Shaginyan L.R., Gorban V.F., Krapivka N.A., Firstov S.A., Kopylov I.F. Properties of coatings from a high-entropy Al – Cr – Fe – Co – Ni – Mo – V alloy obtained by magnetron sputtering // Superhard Materials, 2016, No. 1. - P. 33-44.

9. Firstov S.A., Gorban V.F., Krapivka N.A., Danilenko N.I., Kopylov V.I. The influence of plastic

deformation on the phase composition and properties of high-entropy alloys // Mizhvuzivs'kiy zbirnik "Naukovi notatki", Lutsk, 2016, Issue No. 54. - P. 326-338.

10. Gorban V.F., Krapivka N.A., Firstov S.A. High-entropy alloys - electron concentration - phase composition - lattice parameter - properties // Physics of metals and metal science, 2017, Vol. 118, no. 10. - P. 1017-1029.

11. Yurov V.M., Guchenko S.A., Laurinas V.Ch. The thickness of the surface layer, surface energy and atomic volume of the element // Physicochemical aspects of the study of clusters, nanostructures and nanomaterials, 2018, Issue. 10. - P. 691-699.

12. Yurov V.M., Guchenko S.A. Surface properties of some high-entropy alloys // National Association of Scientists (NAU). 2019, - No. 46. Part 1. - P. 36-38.

13. Yurov V.M., Guchenko S.A. The thickness of the surface layer of high-entropy CrNiTiZrMo coatings // National Association of Scientists (NAU). 2019, - No. 44, Part 1. - P. 40-44.

14. Yurov V.M., Guchenko S.A., Makhanov K.M. Atomic force microscopy of high-entropy coatings // International Journal of Applied and Fundamental Research, 2020, No. 4. - P. 62-67.